# A Fully Integrated Micromachined Magnetic Particle Separator

Chong H. Ahn, *Member, IEEE*, Mark G. Allen, *Member, IEEE*,
William Trimmer, *Member, IEEE*, Yong-Nam Jun, and Shyamsunder Erramilli

***Abstract*—A prototype micromachined magnetic particle separator that can separate magnetic particles from suspended liquid solutions has been realized on a silicon wafer. The requisite magnetic field gradients are generated by integrated inductive components in place of permanent magnets, which yields several advantages in design flexibility, compactness, electrical and optical monitoring, and integration feasibility (thus enabling mass production). Preliminary experiments have been performed on aqueous suspensions of magnetic beads. At 500 mA of dc current, approximately 0.03 Tesla of magnetic flux density is achieved at the gap between the quadrupoles, and the magnetic particles rapidly move toward the quadrupoles, separate from the buffer solution, and clump on the poles. The magnetic particles clumped on the poles are also easily released when the dc current is removed, achieving the primary purpose of a separator. The device shows that micromachined magnetic components have a high potential in biological or biomedical applications, especially in separating small amounts of cells or DNA that are marked with magnetic beads, especially when close monitoring and control of the process is important. [152]**

## I. Introduction

PURIFICATION techniques that are widely used in conventional chemistry such as distillation and crystallization become more difficult to apply as the quantity of material to be purified becomes small. In addition, biological purification requiring separations of biological cells or cell fragments from suspensions can be difficult due to the fragility and ease of aggregation of these materials [1]. The use of magnetic fields for separating out small magnetic particles is a technique that was first proposed by Kolm [2] in order to search for the Dirac magnetic monopole in ocean bottom sediments. While this search proved unsuccessful, the idea of using high magnetic field gradients for separation of particles of small size and magnetization was employed in other areas such as mineral purification, removal of pollutants from water, and coal desulfurization [3]–[5]. Applications in biology were also found in separation of red blood cells from whole blood by using the magnetic moment of hemoglobin in its deoxygenated state [6]–[8]. The most important strength of the magnetic separation techniques is that they provide probably the most rapid and convenient method in separating appropriate particles from diluted suspensions.

In conventional magnetic particle separators as shown in Fig. 1, magnetic particles that are suspended in a fluid are subjected to spatially nonuniform magnetic fields (0.01–0.2 Tesla) produced by an array of arbitrarily positioned, rectangular, rare-earth permanent magnets. In practical separators, in order to achieve a magnetic field gradient that is sufficient to separate the particles, quadrupole or multipole permanent magnet arrangements [9] are adopted and ferromagnetic wires (or wool) are also introduced to generate the required magnetic gradient in an otherwise uniform magnetic field. When the magnetic particles are subjected to the field, magnetic forces are generated on the particles. The particles then migrate and coalesce into the magnetic poles or the ferromagnetic wires. Fig. 2 shows a separator system that generates the magnetic gradient internally in a microtitre well as well as a permanent magnet-pair. The device consists of a nonmagnetic T-shaped frame, which holds removable ferromagnetic wires, a pair of permanent magnets, and a microtitre well to contain a suspension.

In many of the systems, high magnetic field gradient values were achieved by imposing a high background field ($H$) of up to 2 Tesla ($2 \times 10^4$ Gauss) using either a permanent magnet or an electromagnet on a filter of closely packed steel wool of approximately 10 $\mu$m diameter, with a saturation magnetization $M_s \approx 0.8$ Tesla (the convention in the field of magnetics and magnetophoresis is often to use Tesla or Gauss for magnetic fields ($H$) and magnetization ($M$), although strictly speaking $B = \mu(H + M)$, where $B$ is the magnetic flux density and $\mu$ is the permeability). Since the magnitude of the magnetic field inside the steel wool is $\mu(H + M)$, while the field in the empty space between the steel wool is close to the background value of $\mu$H, one can estimate that the gradients generated are of $\mu M_s/a$, where $a$ of approximately 10–100 $\mu$m is a typical size of the gap between the steel wires. Given the saturation magnetization of common ferromagnetic materials of less than 1 Tesla, a typical field gradient produced in such a system is then approximately $10^4$–$10^5$ Tesla/m. Chikov *et al.* [8] took a somewhat different approach to generating

Manuscript received April 26, 1995; revised November 10, 1995. Editor, R. O. Warrington. This work was supported in part by the National Science Foundation under grant ECS-9 117 074.

C. H. Ahn is with the Center for Microelectronic Sensors and MEMS, Department of Electrical and Computer Engineering and Computer Science, University of Cincinnati, Cincinnati, OH 45221-0030 USA.

M. G. Allen is with the Microelectronics Research Center, School of Electrical and Computer Engineering, Georgia Institute of Technology, Atlanta, GA 30322-0250 USA.

W. Trimmer is with Belle Mead Research, Belle Mead, NJ 08502-3218 USA.

Y.-N. Jun is with the Joseph Henry Laboratories, Department of Physics, Princeton University, Princeton, NJ 08544 USA.

S. Erramilli was with the Joseph Henry Laboratories, Department of Physics, Princeton University, Princeton, NJ 08544 USA. He is now with the Department of Physics, Boston University, Boston, MA 02215 USA.

Publisher Item Identifier S 1057-7157(96)06191-4.

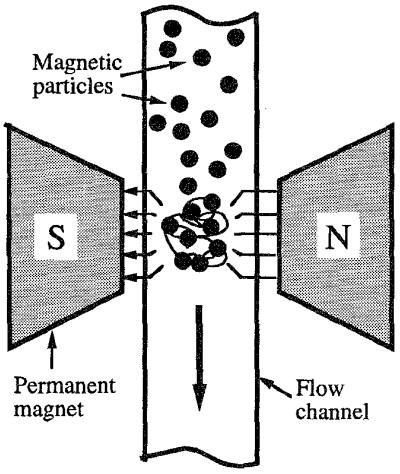


Fig. 1. Schematic diagram of a conventional magnetic separator with permanent magnets.

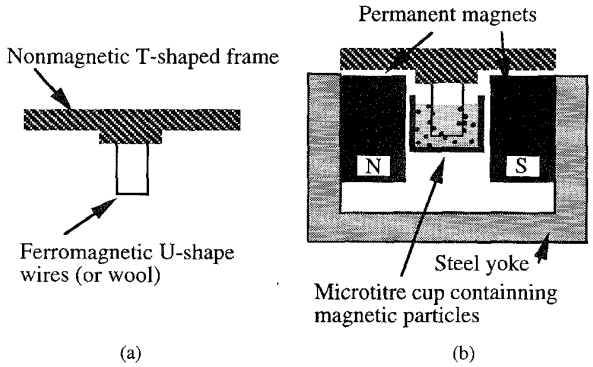


Fig. 2. Practical separator system that generates the magnetic gradient internally in a microtitre well as well as a permanent magnet-pair. (a) T-shaped frame. (b) High gradient magnetic separator.

high gradient magnetic fields, using Stern-Gerlach magnets that are normally used for measuring quantum mechanical spin variables. Recently, a successful biological separator was described, in which fields of 0.04 Tesla (400 Gauss) were applied on a free-flow electrophoresis chamber, producing a gradient of approximately 0.6 Tesla/m (60 Gauss/cm) [10], [11]. Very recently, a new class of porous magnetic materials has been synthesized by processing of random magnetic gels designed specifically for magnetophoresis applications [12].

Most of these approaches, although very successful, have a drawback in that close monitoring of the separation process is difficult by the nature of the filter geometry. Recently, planar-integrated magnetic microactuators [13], [14] that have been realized using planar integrated inductive components [15], [16] exhibit magnetic fields in air gaps (0.2 Tesla) large enough to separate magnetic particles from fluid suspensions. Thus, a prototype integrated magnetic particle separator and manipulator has been reported by C. Ahn *et al.* [17] using the micromachined planar inductive components. The microfabricated device allows us to visually monitor the capture process by a simple optical microscope setup, and the fabrication technology may be further employed to create

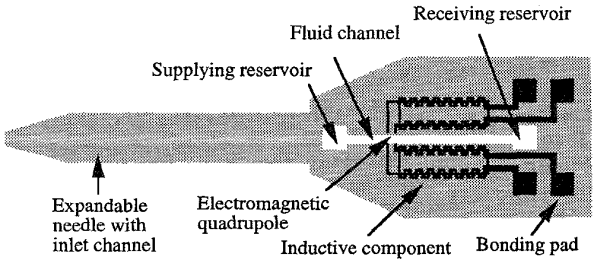


Fig. 3. Schematic diagram of a micromachined magnetic particle separator using integrated inductive components.

devices with which to manipulate magnetic particles with great precision. In this study, an integrated inductive component with completely insulated and integrated coils, as shown in Fig. 3 [16], has been used in place of permanent magnets and yields several advantages in design flexibility, compactness, electrical control, close monitoring, and integration feasibility (thus enabling mass production). In the prototype device, magnetic field gradients realized ($10^2$–$10^3$ Tesla/m) are not as high as those in steel wool filters, but control over the field conformation is possible, and as experiments show, the device is successful in capturing micron-sized magnetic beads out of suspension. The captured particles can be easily eluted from the device by turning off the current to the electromagnet and flushing the particles out. The micromachined version of the separator has a great potential for both biomedical and biomedical applications, envisaging a miniaturized portable or disposable magnetic particle separator.

## II. Principle of Magnetic Separations

Some aspects of the theory behind magnetic particle capture in randomly packed steel wool filters has been worked out in some detail by Watson [18]. Since the geometry of this separator is quite different from his, it is necessary to derive some relevant parameters from the underlying physical principles.

Consider the capture of a cell or a DNA molecule tagged by a magnetic bead, which is the essential application of interest for our system. The biochemical procedure for marking cells and DNA in this manner is well established and has been described in the literature [7], [19]. The magnetic particles of interest are composed of magnetite ($Fe_3O_4$) and are approximately 1 $\mu$m in diameter, with a magnetic moment of the order of $10^{-14}$ Joules/Tesla.

It should be noted that the following calculations assume that magnetic particles have a low density in the suspension. This approximation allows us to neglect interparticle interactions and allows us to work from Newton's equations of motion for a single particle rather than having to resort to the theory of ferrohydrodynamics, where the effect of the magnetic field on the bulk fluid cannot be neglected.

The interaction energy between a magnetic field and a magnetic dipole has the form

$$U = -\vec{\mu} \cdot \vec{B} \tag{1}$$

where $\vec{\mu}$ is the magnetic moment of the particle and $\vec{B}$ is the applied magnetic field. If the applied magnetic field is taken

to be a modest 0.03 Tesla (300 Gauss), the interaction energy is seen to be many orders of magnitude greater than energy $\kappa T$ (where $\kappa$ is Boltzmann's constant and $T$ is temperature in Kelvin) from Brownian motion. Therefore, the magnetic moment of the particle can be considered as being parallel to the field, which means that the dot product reduces to a simple product of the magnitudes of the vectors, $U = -\mu B$.

The magnetic force of attraction felt by the particle is then

$$\vec{F}_{\text{mag}} = -\nabla U = B\nabla\mu + \mu\nabla B. \tag{2}$$

At the magnetic field strengths used, the magnetization of the particles is saturated, and one can assume that $\mu$ is independent of $B$. The particles have a constant dipole moment and the first term can be ignored, and thus the (2) can be rewritten as

$$\vec{F}_{\text{mag}x} = V\chi_\nu \vec{H}\frac{\partial \vec{H}}{\partial x} \tag{3}$$

where $F_{\text{mag}x}$ is the force on the particle in direction $x, V$ is the volume of the particle, $\chi_\nu$ is its magnetic susceptibility per unit volume, $\vec{H}$ is the strength of the magnetic field, and $\partial\vec{H}/\partial x$ is the magnetic field gradient. In (3), the shape of particle is assumed to be spherical and interactions between magnetic particles are not considered. The variable of interest in the trapping force is then seen to be the magnetic field gradient.

In addition to the magnetic force, the biological particle-magnetic bead composite experiences a hydrodynamic drag force. Assuming that there is no macroscopic fluid flow in the suspension, the hydrodynamic interaction may be most simply modeled by Stokes's law for the drag on a sphere

$$\vec{F}_{\text{drag}} = -6\pi\eta R\vec{\nu} \tag{4}$$

with the rough assumption that the cell–bead composite has the approximate shape of a sphere of radius $R$, where $\eta$ is the solution viscosity and $\vec{\nu}$ is the particle velocity. The drag force on a DNA molecule has the form

$$\vec{F}_{\text{drag}} = -6\pi\eta L\vec{\nu} \tag{5}$$

where $L$ is the length of the polymer [20].

The drag on the magnetic bead–DNA system can be modeled by this term if the polymer is long enough. In both cases, the force is a velocity-dependent damping term. The effect of gravity is assumed to be negligibly small due to the extremely small size of the particles. In addition, the Reynolds' number of the system is low (approximately 0.01), which allows us to neglect the inertia term in Newton's law [21]. The resulting equation of motion (for a spherical particle) is

$$\mu\nabla B = -6\pi\eta R\frac{d\vec{x}}{dt}, \tag{6}$$

which can be integrated with the assumption that the gradient of the field is constant to yield the time-dependent equation for the position

$$\vec{x} = \vec{x}_0 + \vec{\nu}_{\text{sep}}t \tag{7}$$

where the velocity of separation $\vec{\nu}_{\text{sep}}$ is given by

$$\vec{\nu}_{\text{sep}} = -\mu\nabla B/f(\eta). \tag{8}$$

For a spherical particle of radius $R$, $f(\eta)$ is often assumed to be given by Stokes's law and is set to $6\pi\eta R$. This velocity can be maximized by reducing the drag forces on the bead–cell composite and/or increasing the magnetic force on the magnetic beads. In practice, the drag forces are fixed, so trapping speed can be improved only through the magnetics of the system. When separation velocity is worked out for the microseparator using appropriate values, it is seen to be on the order of 1 mm/s, which is a value consistent with our experimental observations [22].

## III. Design

From the above analysis, it is clear that the parameter to be maximized is the gradient of $B$, while maintaining a value of $H$ that is large enough to ensure complete alignment and saturation of the particles. Desirable design parameters are then seen to be: 1) reasonably moderate field values (approximately 0.01 Tesla) that are enough to ensure full alignment and saturation; 2) high field gradients approximately $10^4$ Tesla/m; 3) ease of coupling to fluid flow; and 4) compatibility with optical microscope stage for easy visual monitoring.

To realize an integrated separator on a silicon wafer while achieving the design parameters described above, all the functions of the hybrid components used in the conventional separator should be integrated together on the substrate. Thin film electromagnets with integrated coils have been used in place of the permanent magnets and a flow channel to guide the magnetic fluid suspension has been introduced in place of the vessel containing the fluid. The integrated device concept is shown in Fig. 4, where two integrated inductors are placed between the flow channel used to guide magnetic fluid. In this separator, suspended magnetic particles are subjected to the magnetic fields (generated by the integrated inductive components) and field gradients (generated from the component pole geometries) and, thus, are forced to move from the suspension to the surface of electromagnetic poles. The collected particles on the surface of the poles can be released by removing the current excitation of the electromagnets.

The achievable magnetic field strength $H$ depends on the performance of the inductive component, which is limited by the allowable size and planar fabrication processes. The device discussed is designed to be implemented in an area of 2 mm × 3 mm. The achievable magnetic field strength is strongly affected by the width of the flow channel that acts as an air gap in magnetic circuits. From the point view of reluctance in the magnetic circuit, a narrower width of the channel would be preferred, but it should have an appropriate width since the flow rate of a viscous magnetic fluid will be limited as the channel width is reduced [23], [24]. Thus, in this

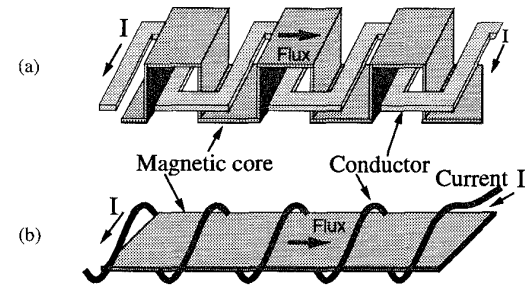


Fig. 4. Integrated toroidal-meander-type inductor. (a) Schematic diagram of the integrated toroidal-meander-type inductor. (b) Analogous structure to a conventional inductor.

device, the width of the flow channel is designed to be 100 $\mu$m, which allows an appropriate flow rate for the magnetic fluid as well as provide compatibility with optical microscope stage for easy visual monitoring, while a magnetic flux density of 0.03 Tesla can be achieved in the air gap by flowing 500 mA of dc current through the coil conductors.

In contrast to the conventional separator, the magnetic core in this device has a shape of a bar and the electromagnet poles located at the end of the core are almost similar to the tip of a needle in shape. Thus, a high magnetic field gradient will be generated at the tip of the poles. In this small pole geometry, in order to achieve a high magnetic field gradient in the air gap, appropriate positioning and allocation of the poles is a dominant design consideration. An electromagnet quadrupole is adopted using two inductive components placed at both sides of the channel, and thus two combinations of quadrupoles can be produced flexibly by switching dc excitation polarities at the coils as shown in Fig. 5. In order to achieve high magnetic field gradient at the tip of the poles, magnetic flux leakages should be prevented between cores that are placed in proximity to each other, ensuring that as much of the flux as possible is concentrated at the tip of the poles. For this purpose, a magnetic shield layer as shown in Fig. 6 is introduced, which reduces the flux leakage at the cores and maximizes the flux at the pole tips.

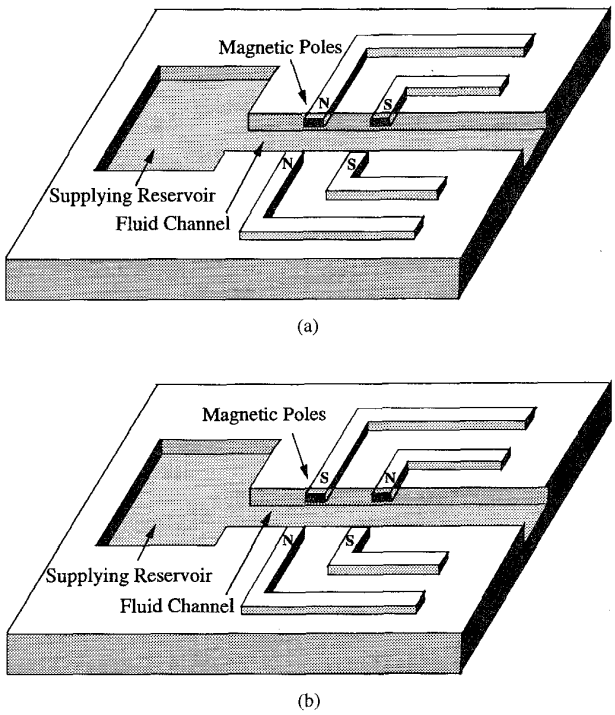


Fig. 5. Two different quadrupoles generated by using different dc excitations in coils. (a) N-N-S-S pole combination. (b) N-S-N-S pole combination.

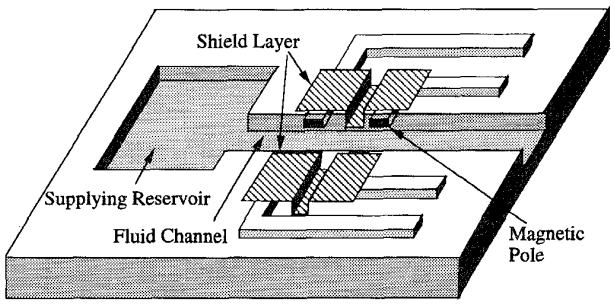


Fig. 6. Schematic diagram of quadrupole with a magnetic shield layer.

## IV. Fabrication

A meander-type integrated inductive component [15], [16] was fabricated using a polyimide multilevel metal interconnection technique, in which an electroplated high permeability Ni(81%)-Fe(19%) permalloy was used as the magnetic material. A brief fabrication process of this separator is shown in Fig. 7. The process started with 2-in. $\langle 100 \rangle$ silicon wafers as a substrate, onto which 0.3 $\mu$m of PECVD silicon nitride was deposited. Onto this substrate, titanium (1000 Å) /copper (2000 Å)/chromium (700 Å) layers were deposited using electron-beam evaporation to form both a seed layer for electroplating and a bottom layer for the flow channel. Polyimide (Dupont PI-2611) was then spun on the wafer in multiple coats to build electroplating molds for the bottom magnetic core. After the deposition of all coats, the polyimide was cured at 300°C for 1 h in nitrogen, yielding an after-cure thickness of 40 $\mu$m. Holes that contained bottom magnetic cores were etched in this polyimide using a 100% $O_2$ plasma etch and an aluminum hard mask until the titanium/copper/chrome seed layer was exposed. The electroplating molds were then filled with Ni(81%)-Fe(19%) permalloy using standard electroplating techniques [25]. To build a magnetic shield layer, a shield trench was made around the quadrupole region using the same dry-etch process described above. A dc-sputtered titanium (500 Å) layer was deposited and then patterned over the region, which requires the magnetic shield. In order to insulate the bottom magnetic core and the shield layer from the conductor coil, polyimide was spin-coated (as above) and hard-cured at 300°C for 1 h. To construct a thick planar meander conductor coil, copper was plated on a chromium (500Å)/copper (2000 Å)/chromium (700 Å) seed layer through a thick photoresist mold, in which a 70-$\mu$m-wide copper plating mold was formed in 8- $\mu$m-thick positive photoresist. The copper conductors were plated through the defined molds using standard electroplating techniques [15]. Upon completion of the electroplating,

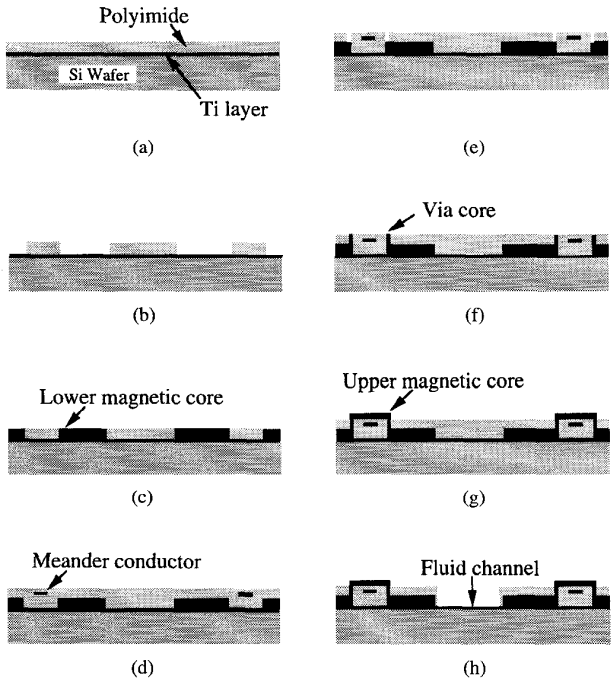


Fig. 7. Fabrication steps of the micromachined separator: (a) polyimide deposition; (b) dry-etching lower core molds; (c) plating lower core and magnetic shield layer deposition; (d) conductor deposition; (e) dry-etching via molds; (f) plating magnetic vias; (g) plating upper core; (h) dry-etching fluid channel.

the photoresist was removed with acetone and the copper seed layer was etched in a sulfuric-acid-based copper etching solution.

One coat of polyimide approximately 10 $\mu$m in thickness was deposited for conductor insulation and cured as described above. Via holes were dry-etched through the polyimide layer between the meander conductors using 100% oxygen plasma and an aluminum hard mask. The vias were filled with nickel–iron permalloy using the electroplating bath and conditions described previously. After completing the via electroplating, top magnetic cores were processed on the same level using the same process used for conductor plating with thick positive photoresist. Upon completion of the top core electroplating, the photoresist and seed layer were removed. The final thickness of the device relative to the substrate was approximately 90 $\mu$m. The details of the inductive component fabrication are covered in [16].

Finally, fluid flow channel and bonding pads were opened in the polyimide layers by using the via etch process sequence described above. To remove the copper/chrome layer located on the bottom of the channel, the structure was dry-etched to the bottom achieving 90 $\mu$m of channel depth, and the copper/chrome layer was then selectively wet etched. A bright titanium layer, which can serve as a mirror for the optical monitoring, is thereby exposed on the bottom of the channel. Fig. 8 shows a photomicrograph of the fabricated particle separator with a size of 2 mm $\times$ 3 mm. A scanning electron micrograph (SEM) of the quadrupole region is shown in Fig. 9, where the magnetic shield layer is not included.

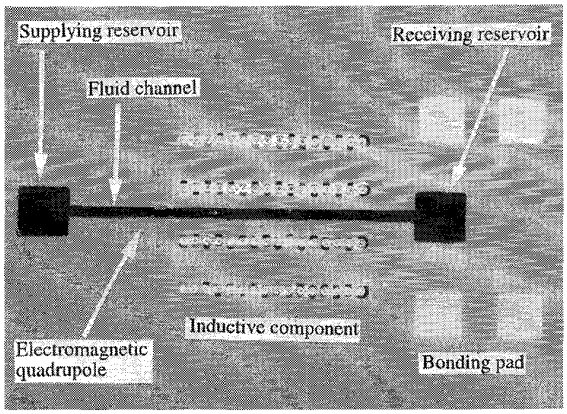


Fig. 8. Photomicrograph of the fabricated particle separator.

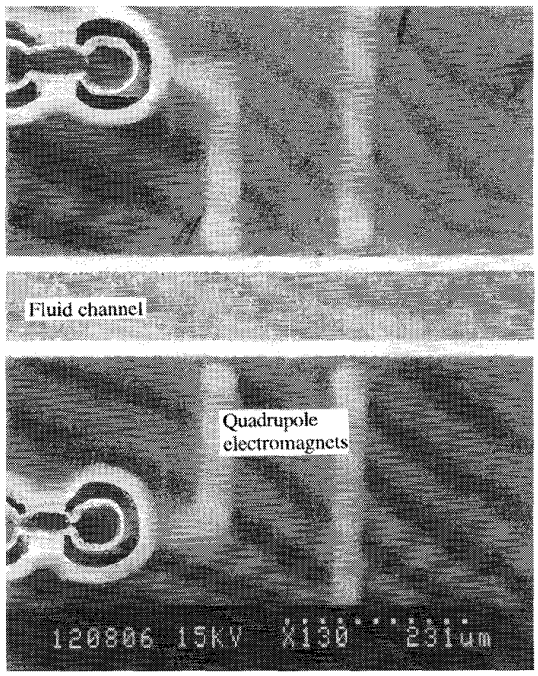


Fig. 9. Scanning electron micrograph (SEM) of the quadrupole, where the magnetic shield layer is not included.

## V. Experimental Results and Discussion

The magnetic particles used in this experiment are commercially available superparamagnetic particles (Estapor carboxylate-modified superparamagnetic particles, Bangs Laboratories, Inc.) that are supplied as a aqueous dispersion with 60% solid content of magnetite. This magnetic particle consists of a ferrite crystal (magnetite) with median diameters of 0.8–1.3 $\mu$m. The magnetic particle density is 2.2 g/ml. The particles are surrounded by the usual polystyrene and carboxylic acid-modified shell to isolate iron from the surface, so that they can be used for adsorption as well as covalent attachment.

Separation tests can be performed either by flowing a suspension through the channel or by dipping the quadrupoles

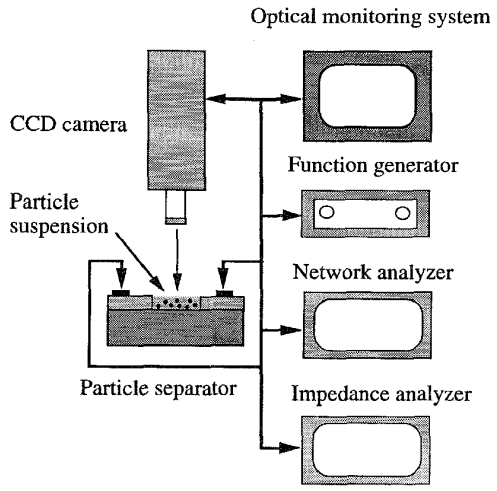


Fig. 10. Electrical and optical test system. Particle separations and movements can be monitored easily using this electrical and optical system while the particle separations proceed.

of the separator into the suspension. It was mentioned earlier that the major advantages of this separator come from a simplicity of separation steps, an ease of device handling, and a flexibility of optical monitoring as compared with the conventional hybrid separator in Fig. 2. As described in Fig. 10, the particle separations and movements can be monitored easily using an optical system (CCD or laser scanning techniques) while the particle separations proceed.

In this study, the magnetic suspension is placed first in a syringe for handling convenience. To begin the experiment, approximately ten drops of suspension are applied to the supplying reservoir resulting in fluid flow through the channel. Because of the surface tension of liquid, the suspension is able to be confined inside the supplying reservoir at the beginning, and then it continuously flows toward the receiving reservoir through the channel until the fluid level between the two reservoirs is equal. While the suspension flows through the channel, the separation experiment is performed. With no current applied to the coils (i.e., without a magnetic field), no significant sedimentation or attachment of dispersed particles on the poles occurs even over a time span of several hours. An initial movement of magnetic particles is observed through a microscope when the dc current in coils reaches 100 mA. To achieve a magnetic flux density of 0.03 Tesla at the air gap, it is estimated that the applied coil current should be at least 500 mA. When 0.8 V of dc voltage is applied to each inductor, resulting in a current flow of 500 mA, the particles move rapidly toward the quadrupole, separate from the buffer solution, and clump on the poles. Upon removal of the current, the particles are immediately redispersed from the poles without clumping (from Brownian motion). While the dc voltage is continuously applied to the inductor, however, the separator that is holding the particles can be moved and emerged into a new buffer solution, and then the particles can easily be released into the new buffer solution by removing the dc excitation.

The separation velocity of approximately 1 mm/s was measured using the video camera (CCD based) and a frame grabbler to estimate the speeds [26]. There is a variation in the speeds due to the nonuniformity of the field gradient as well as a nonuniformity in the particle magnetic moment. A detailed comparison between the theory and the measurement is really difficult for these two reasons; the measured separation velocity, however, shows a rough agreement with the estimated value in the order of magnitude.

As shown in Fig. 5, two different combinations of electromagnet quadrupole can be produced by changing the polarities of the dc excitation in the coils. The effect of the magnetic polarity on the separation was qualitatively assessed by applying 500 mA of dc current to each inductor for 10 s for both magnetic polarities. In the separation of the magnetic particles using dc excitation, any significant difference between without and with the shield layer was not observed. This would be due to the easy penetration of dc magnetic flux through the thin titanium metal film. Thus, to improve the magnetic shielding for the dc excitation, a ferromagnetic film should be deposited as the shielding layer. The results of this experiment are shown in Fig. 11, where the separated particles on the poles of polarity N-N-S-S and N-S-N-S quadrupole (clockwise in series) are shown. From Fig. 11, it is qualitatively observed that the magnetic particles are attracted more strongly from the N-N-S-S pole combination than the N-S-N-S combination, which may be due to a stronger magnetic field gradient attained from the N-N-S-S pole combination because of differing magnetic flux paths.

The inductance of a inductor usually varies as the reluctance of the magnetic path is varied. As particles are clumped on the poles, the reluctance in the air gap between poles will vary, resulting in a change in the inductance of the drive component. If this inductance variation as a function of separation time and current can be detected, the amount of separated particles may be approximately evaluated from the inductor geometry and the magnetic properties of the particles. This *in-situ* evaluation of particle separation efficiency is currently under development.

## VI. Conclusion

A micromachined magnetic particle manipulator that can be used to influence magnetic particles suspended in liquid solutions has been realized on a silicon wafer. A meander-type integrated inductor with fully integrated and insulated coils has been used as a basic component for the manipulator electromagnet. One potential application of this manipulator is magnetic particle separation from solution. When 500 mA of dc current with a drive voltage less than 1 V is applied to each inductor, particle separation is observed. The magnetic particles clumped on the surface of electromagnet poles can be released and resuspended easily by removing the applied current. This separator can be used repeatedly for different separations after washing using acetone- and methanol-based cleaning steps. Simple tests using this prototypical device show that application of microfabrication technology to magnetic particle separation is a promising field of research with

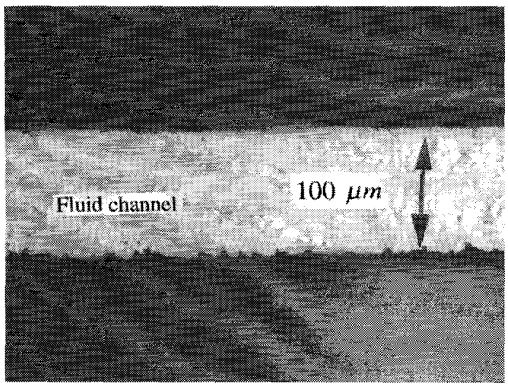


(a)

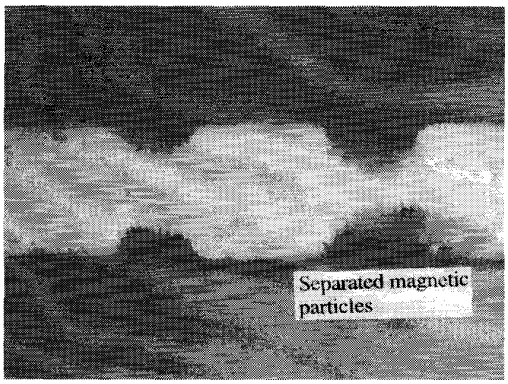


(b)

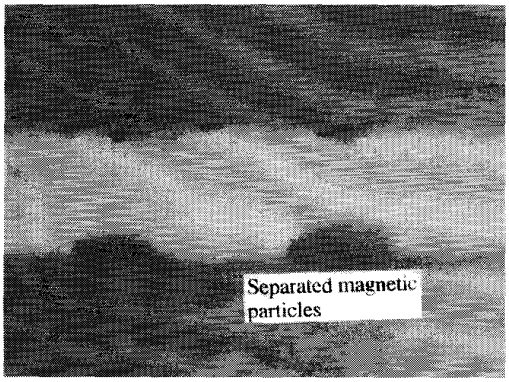


(c)

Fig. 11. Magnetic particles that are collected on the edges of magnetic electrodes: (a) before applying current; (b) 10 seconds after applying current at N-N-S-S quadrupoles; and (c) 10 s after applying current at N-S-N-S quadrupoles. The magnetic particle size is approximately 0.8–1.3 $\mu$m and the width of channel is 100 $\mu$m.

many possible applications in solving biological or biomedical problems.

## ACKNOWLEDGMENT

Microfabrication was carried out at the Microelectronics Research Center (MiRC) of the Georgia Institute of Technology. The authors would also like to acknowledge DuPont, OCG Microelectronic Materials for their donations of polyimide, and Lake Shore Cryotronics, Inc. for their assistance in measurements of the magnetic properties of permalloy thin films.

## REFERENCES

[1] G. M. Whitesides, R. J. Kazlauskas, and L. Josephson, "Magnetic separations in biotechnology," *Trends in Biotechnology*, vol. 1, no. 5, pp. 144–148, 1983.
[2] K. Kolm, F. Villa, and A. Odian, "Search for magnetic monopoles," *Phys. Rev. D*, vol. 4, p. 1285, 1971.
[3] D. Kelland, "High gradient magnetic separation applied to mineral beneficiation," *IEEE Trans. Magn.*, vol. MAG-9, no. 3, p. 307, 1973.
[4] S. Trindade and H. Kolm, "Magnetic desulferization of coal," *IEEE Trans. Magn.*, vol. MAG-9, no. 3, p. 310, 1973.
[5] C. de Latour, "Magnetic separation in water pollution control," *IEEE Trans. Magn.*, vol. MAG-9, no. 3, p. 314, 1973.
[6] D. Melville, F. Paul, and S. Roath, "High gradient magnetic separation of red cells from whole blood," *IEEE Trans. Magn.*, vol. MAG-11, no. 6, p. 1701, 1975.
[7] S. Roath, A. Smith, and J. H. P. Watson, "High gradient magnetic separation in blood and bone marrow processing,"*J. Mag. Mag. Mater.*, no. 85, p. 285, 1990.
[8] V. Chikov, A. Kuznetsov, A. Shapiro, S. Winoto-Morbach, and W. Mueller-Ruchholtz, "Single cell magnetophoresis and its diagnostic value," *J. Mag. Mag. Mater.*, no. 122, p. 367, 1993.
[9] P. A. Liberti and B. P. Feeley, "Analytical and process scale cell separation with bioreceptor ferrofluid and high gradient magnetic separator," in *Proc. 119th National Meet. American Chemical Society*, Boston, MA, Apr. 22–27, 1990, pp. 269–288.
[10] R. Hartig, M. Hausmann, J. Schmitt, D. Herrmann, M. Riedmiller, and C. Cremer, "Preparative continuous separation of biological particles by means of free-flow magnetophoresis in a free flow electrophoresis Chamber," *Electrophoresis,* no. 13, p. 674, 1992.
[11] S. Miltenyi, W. Muller, W. Weichel, and A. Radbruch, "High-gradient magnetic cell-separation with MACS," *Cytometry*, vol. 11, no. 2, p. 231, 1990.
[12] Y.-N. Jun, D. Dabbs, I. A. Aksay, and S. Erramilli, "Processing of monolithic magnetic gels for magnetophoresis," *Langmuir*, Sept 1994, in review.
[13] C. H. Ahn and M. G. Allen, "A fully integrated surface micromachined magnetic microactuator with a multilevel meander magnetic core," *J. Microelectromech. Syst.*, vol. 2, no. 1, pp. 15–22, 1993.
[14] C. H. Ahn, Y. J. Kim, and M. G. Allen, "A planar variable reluctance magnetic micromotor with fully integrated stators," *J. Microelectromech. Syst.*, vol. 2, no. 4, 1993.
[15] C. H. Ahn, "Micromachined components as integrated inductors and magnetic microactuators," Ph.D. Dissertation, Georgia Institute of Technology, Atlanta, GA, 1993.
[16] C. H. Ahn and M. G. Allen, "A new toroidal-meander type integrated inductor with a multilevel meander magnetic core," *IEEE Trans. Magn.*, vol. 30, no. 1, pp. 73–79, 1994.
[17] ——, "A fully integrated micromachined magnetic particle manipulator and separator," in *Proc. IEEE Micro Electro Mechanical Systems Workshop*, Japan, Jan. 25–28, 1994, pp. 35–41.
[18] J. H. P. Watson, "Magnetic Filtration," *J. Appl. Phys.*, vol. 44, no. 9, p. 4209, 1973.
[19] R. Zimmermann and E. Cox, "DNA stretching on functionalized gold surfaces," *Nucleic Acids Research*, vol. 22, no. 3, p. 492, 1994.
[20] W. Volkmuth, T. Duke, M. Wu, R. Austin, and A. Szabo, "DNA electrodiffusion in a 2D array of posts," *Phys. Rev. Lett.*, vol. 72, no. 13, p. 2117, 1994.
[21] The characteristic velocity is taken to be 0.1 cm/s, the length taken to be 10 $\mu$ and the kinematic viscosity is 0.01 in cgs units.
[22] The assumptions are: aqueous medium, gradient 10000 Gauss/cm and $mu$ on the order of $10^{10}$ erg/Gauss (all in cgs units).
[23] D. Sobek, A. M. Young, M. L. Gray, and S. D. Senturia, "A microfabricated flow chamber for optical measurements in fluids," in *Proc. IEEE Microelectromechanical Systems Workshop*, Feb. 7–10, 1993, pp. 219–224.
[24] S. W. Charles, "Magnetic fluid (ferrofluids)," in *Proc. Int. Workshop on Studies of Magnetic Properties of Fine Particles*, Rome, Italy, Nov. 4–8, 1991, pp. 267–276.
[25] I. W. Wolf, "Electrodeposition of magnetic materials," *J. Appl. Phys.*, vol. 33, no. 3, pp. 1152–1159, 1962.
[26] Y.-N. Jun, Senior Thesis, Princeton Univ., 1994.

**Chong H. Ahn** (S'90–M'91) received the B.S. degree in electrical engineering from Inha University, South Korea, in 1980. In 1983, he received the M.S. degree in electrical engineering from Seoul National University, South Korea. He received the Ph.D. degree in electrical and computer engineering from the Georgia Institute of Technology, Atlanta, in 1993.

He was an Assistant Professor in the Department of Computer Engineering at Inha Technical Jr. College from 1983 to 1987. From 1993 through 1994, he worked as a postdoctoral Fellow at the Georgia Institute of Technology and then at IBM T. J. Watson Research Center, Yorktown Heights, NY. Since 1994, he has been an Assistant Professor of Electrical and Computer Engineering and Computer Science at the University of Cincinnati, OH. His research interests include the development, design, fabrication, and characterization of micromachined sensors and actuators, nondestructive eddy–current sensors, magnetic field-based biosensors, microvalves and micropumps, microfluidic systems for biological, chemical, and environmental applications, electrooptical multichip modules (OE-MCM) and I/O coupler, and micromachining techniques for magnetic MEMS.

**Mark G. Allen** (M'89) received the B.A. degree in chemistry, the B.S.E. degree in chemical engineering, and the B.S.E. degree in electrical engineering from the University of Pennsylvania, Philadelphia, in 1984 and the S.M. and Ph.D. degrees from the Massachusetts Institute of Technology, Cambridge, in 1986 and 1989, respectively.

Since 1989, he has been on the faculty of the School of Electrical and Computer Engineering at the Georgia Institute of Technology, Atlanta, where he is currently an Associate Professor. His research area is in micromachining, with special emphasis on magnetic materials and devices, micromachining issues in electronic packaging, and micromachined fluidic devices.

**William Trimmer** (M'86) received the B.A. degree in 1966 from Occidental College, Los Angeles, CA, and the Ph.D. degree in 1972 in experimental relativity from Wesleyan University, Middletown, CT, where he was Graduate Student Body President.

He taught at Montclair State College, Montclair, NJ, and The College of Wooster, Wooster, OH, where he was Department Chairman. He worked in Singer's Corporate Laboratory developing displays for sewing machines and at Johnson & Johnson developing acoustical imaging systems for early detection of breast cancer. In 1982 he joined AT&T Bell Laboratories. One of his programs developed a robotic system to test the small and fragile chips used in fiber-optic systems. In 1984, he started a program on micro robots that evolved into a research effort in micromechanics and MEMS. In 1990 he started Belle Mead Research (BMR), Belle Mead, NJ. BMR develops products involving micromechanics, helps facilitate new micromechanics businesses, and conducts science and engineering research programs.

Dr. Trimmer co-chaired the first workshop on micromechanics, called Micro Robots and Teleoperators, in 1987—the initial workshop in the international series of MEMS workshops. In 1989 he started, and was Editor, of the Micromechanics section of the *Sensors and Actuators*. Next, he organized the first joint IEEE and ASME publication, the JOURNAL OF MICROELECTROMECHANICAL SYSTEMS, of which he is presently the Editor.

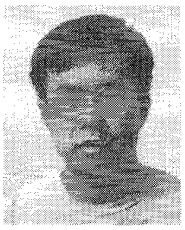

**Yong-Nam Jun** was born in Pusan, Korea, on April 23, 1974. He received the A.B. degree with honors in physics from Princeton University in 1994, with a certificate in applied and computational mathematics. His senior thesis research topic was magnetophoresis.

Currently, he is a candidate for the Ph.D. degree in physics at the California Institute of Technology, Pasadena (will receive M.S. degree in 1996), studying problems relating to computational neurobiology.

Mr. Jun is a member of Phi Beta Kappa and Sigma Xi.

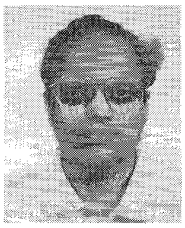

**Shyamsunder Erramilli** received the Ph.D. degree in physics from the University of Illinois, Urbana, working with Hans Frauenfelder.

He joined the faculty of the Physics Department at Princeton University, Princeton, NJ, where he taught for ten years. His research interests have been the application of imaging techniques in biological physics, using x-ray diffraction and high-pressure to study biological systems and, most recently, developing new forms of infrared microscopy. In 1996, he received a joint appointment in Photonics and Physics to Boston University, MA.

Dr. Erramilli received the DuPont Young Professor award in 1995.